Spin versus lattice polaron: Prediction for electron-doped $CaMnO_3$

Yiing-Rei Chen and Philip B. Allen
Department of Physics and Astronomy, State University of New York, Stony Brook, New York 11794-3800
(Received 23 January 2001; revised manuscript received 23 April 2001; published 11 July 2001)

$CaMnO_3$ is a simple bipartite antiferromagnet (AF) that can be continuously electron doped up to $LaMnO_3$. Electrons enter the doubly degenerate E_g subshell with spins aligned to the $S=\frac{3}{2}$ core of $Mn^{4+}(T_{2g}^{3\uparrow})$. We take the Hubbard and Hund energies to be effectively infinite. Our model Hamiltonian has two E_g orbitals per Mn atom, nearest-neighbor hopping, nearest neighbor exchange coupling of the $S=\frac{3}{2}$ cores, and electron-phonon coupling of Mn orbitals to adjacent oxygen atoms. We solve this model for light doping. Electrons are confined in local ferromagnetic (FM) regions (spin polarons) where there proceeds an interesting competition between spin polarization (spin polarons), which enlarges the polaron, and lattice polarization (Jahn-Teller polarons), which makes it smaller. A symmetric seven-atom ferromagnetic cluster (Mn_7^{27+}) is the stable result, with a net spin $S=2$ relative to the undoped AF. The distorted oxygen positions around the electron are predicted. The possibility that two electrons will form a bipolaron has been considered. A fairly modest Coulomb repulsion $U_c=0.98|t|$ (where $t\approx-0.75$ eV) will destroy any simple bipolaron. Therefore we do not expect phase separation to occur. The model predicts a critical doping $x\simeq0.045$ where the polaronic insulator becomes unstable relative to a FM metal.

DOI: 10.1103/PhysRevB.64.064401 PACS number(s): 75.30.Vn, 75.50.Ee, 71.38.Ht

I. INTRODUCTION

$CaMnO_3$ is a bipartite (G-type) antiferromagnetic (AF) insulator[1] with a Néel temperature $T_N=125$ K and almost perfect cubic perovskite crystal structure. There is not a large amount of literature on this material. It deserves attention as a particularly simple case of an AF insulator that can be electron doped. The (T,x) phase diagram[2,3] of the $Ca_{1-x}La_xMnO_3$ series has attracted attention because of the fascinating interplay of spin order, orbital order, and metallic versus insulating transport. ''Colossal magnetoresistance'' occurring at concentration $x\approx0.65$ and $T\approx250$ K is the most dramatic manifestation.[4] For small x, magnetization and conductivity measurements[5,6] suggest local ferromagnetic (FM) regions or ''spin polarons'' in the range $0.02<x<0.06$. In this paper we use a model for pure $CaMnO_3$, the $x=0$ end member, and predict its behavior under light doping $x\ll1$. We keep T equal to 0 and neglect lattice zero-point energy, but allow both spin and lattice coordinates to relax.

Our main question is, what is the ground state of an excess electron in $CaMnO_3$? The answer to this question will also apply to lightly doped $CaMnO_3$ provided the doped state is homogeneous. Our model has four parameters. (1) The bandwidth parameter t governs the effective Mn E_g electron hopping between Mn^{3+} and Mn^{4+} through the intervening oxygen. The spins of the two Mn ions must be parallel as in the usual ''double-exchange'' model.[7,8] (2) The magnetic exchange parameter J couples spins of first-neighbor Mn ions, due to virtual hopping of T_{2g} electrons. (3) The electron-phonon coupling constant g describes interactions between Mn E_g orbitals and the six nearest oxygen atoms. (4) Oxygen displacements u are opposed by the restoring force $-Ku$, where $\omega=\sqrt{K/M}$ is an Einstein frequency assigned to oxygen vibrations along the bonds. There are two important dimensionless parameters. Spin polarons[9] are controlled by the ratio $\beta=t/JS^2$. Jahn-Teller (JT) lattice polarons[10] are controlled by the parameter $\Gamma=g^2/Kt$.[11] Balancing these competing effects, we find the most favorable local FM spin arrangement, lattice distortion, and electron wave function. As doping increases, we predict a transition from polaronic insulator to FM metal.

II. MODEL HAMILTONIAN

The Mn^{4+} ion in $CaMnO_3$ has a configuration $3d^3$, i.e., the three spin-aligned T_{2g} states (xy,yz,zx) are filled with electrons, while the two spin-aligned E_g states $[\psi_2=(x^2-y^2)/\sqrt{3},\psi_3=3z^2-r^2]$ are empty and lie above by the crystal-field splitting. The empty opposite-spin T_{2g} states are split to even higher energy by the Hund term J_H. Light electron doping puts carriers into the doubly degenerate E_g level. Hopping of the $(dd\pi)$-type occurs from T_{2g} to T_{2g} and of the $(dd\sigma)$-type from E_g to E_g, but no E_g to T_{2g} hopping matrix element exists because of the simple cubic structure. Virtual T_{2g} hopping[12] (at the cost of Hubbard energy U) gains delocalization energy if adjacent spins are antiparallel. This gives an $S=\frac{3}{2}$ antiferromagnetic Heisenberg Hamiltonian with exchange coupling $J=2(dd\pi)^2/U$,[13] U being large compared with $(dd\pi)$,[14] and agrees with the experimentally observed magnetic structure of pure $CaMnO_3$. The ground state has $\uparrow$ spins on the A sublattice [when $\exp(i\vec{Q}\cdot\vec{l})=1$, where $\vec{l}$ labels the Mn sites] and $\downarrow$ spins on the B sublattice [when $\exp(i\vec{Q}\cdot\vec{l})=-1$] with $\vec{Q}=(\pi,\pi,\pi)$.

Ignoring for now the electron-phonon terms, the Hamiltonian for an excess electron is $\mathcal{H}=\mathcal{H}_t+\mathcal{H}_J$. The first term contains hopping of Mn E_g electrons to nearest neighbors,

$$\mathcal{H}_t=t\sum_{l,\pm}[L(\vec{l},\vec{l}\pm\hat{z})c_3^\dagger(\vec{l}\pm\hat{z})c_3(\vec{l}) + \text{rotations to } \hat{x},\hat{y} \text{ directions}], \quad (1)$$

$$L(1,2)=\cos\frac{\theta_1}{2}\cos\frac{\theta_2}{2}+\sin\frac{\theta_1}{2}\sin\frac{\theta_2}{2}e^{-i(\phi_1-\phi_2)}. \quad (2)$$

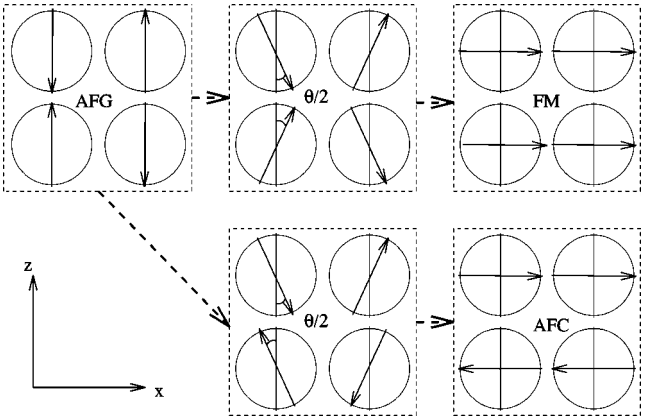

FIG. 1. Schematic spin structures for the antiferromagnetic *G* (AFG), ferromagnetic (FM), and antiferromagnetic *C* (AFC) structures and interpolating canted structures.

Here $c_3(\vec{l})$ destroys an electron state $\psi_3(\vec{r}-\vec{l})$ on the Mn atom at $\vec{l}$, $\vec{l}\pm\hat{z}$ labels the Mn neighbors above and below the one at site $\vec{l}$, and t is the $(dd\sigma)$ integral from the Slater-Koster two-center theory.[15] We use a value $t=-0.75$ eV obtained from fitting the band structure of $CaMnO_3$ (Refs. 16 and 17) (see Sec. III). The factor $L(1,2)$ comes from locally rotating the axis of spin quantization for the ith E_g electron into the direction (θ_i,ϕ_i) of the i^{th} $S=\frac{3}{2}$ core spin, treating the angles (θ_i,ϕ_i) as classical parameters and discarding from the Hilbert space the state with spin opposite to the core spin [i.e., assuming $J_H\rightarrow\infty$ (Refs. 17 and 18). In this paper, we usually take the spins to be perfectly ordered at $T=0$, that is, $\theta=\theta_1-\theta_2$ equals 0 or π, corresponding to $L(1,2)$ equal to 1 or 0 for FM or AF oriented neighbors. We will also consider uniformly canted states where a relative angle $\theta=\pi-\theta_0$ occurs (with $\phi_1-\phi_2=0$), so that L takes the value $\sin(\theta_0/2)$. These spin orientations are shown in Fig. 1.

The rotation of ψ_3 to the $\hat{x}$ axis is $(-\psi_3+\sqrt{3}\psi_2)/2=3x^2-r^2$, and to the $\hat{y}$ axis it is $(-\psi_3-\sqrt{3}\psi_2)/2=3y^2-r^2$. Using these, we rewrite $\mathcal{H}_t$ in the usual orthonormal basis (ψ_2,ψ_3),

$$\mathcal{H}_t=t\sum_{l,\delta=x,y,z}(c_2^\dagger(\vec{l})\quad c_3^\dagger(\vec{l}))\mathsf{T}_\delta\begin{pmatrix}c_2(\vec{l}\pm\hat{\delta})\\ c_3(\vec{l}\pm\hat{\delta})\end{pmatrix},\qquad(3)$$

where it is understood that the hopping only operates between parallel spin Mn atoms. The hopping matrices are

$$\mathsf{T}_x=\begin{pmatrix}\frac{3}{4} & -\frac{\sqrt{3}}{4}\\ -\frac{\sqrt{3}}{4} & \frac{1}{4}\end{pmatrix},\quad \mathsf{T}_y=\begin{pmatrix}\frac{3}{4} & \frac{\sqrt{3}}{4}\\ \frac{\sqrt{3}}{4} & \frac{1}{4}\end{pmatrix},$$

$$\mathsf{T}_z=\begin{pmatrix}0 & 0\\ 0 & 1\end{pmatrix}.\qquad(4)$$

The $\mathcal{H}_J$ term is the AF nearest-neighbor T_{2g} exchange

$$\mathcal{H}_J=\sum_{\langle l,l'\rangle}J\vec{S}(\vec{l})\cdot\vec{S}(\vec{l}').\qquad(5)$$

Mean-field theory gives the value $JS^2=3.23$ meV for the exchange coupling [we use a quantum treatment for spin $\frac{3}{2}$ and the measured Néel temperature $T_N=125$ K (Ref. 19)]. Corrections to mean-field theory for the Heisenberg antiferromagnet[20–22] increase JS^2 to 4.74 meV. This gives $t/JS^2=158$, with a probable uncertainty of 10%. The phonon parts of the Hamiltonian are given in Sec. V.

III. UNIFORM SOLUTIONS

First consider the hypothetical case of a uniform FM spin order. Then a doped-in electron could hop without paying a Hund penalty, and extended Bloch states would form with wave functions

$$\Psi_k=d_2\frac{1}{\sqrt{N}}\sum_l e^{i\vec{k}\cdot\vec{l}}\psi_2(\vec{l})+d_3\frac{1}{\sqrt{N}}\sum_l e^{i\vec{k}\cdot\vec{l}}\psi_3(\vec{l}),\quad(6)$$

where d_2,d_3 are coefficients. Diagonalizing Eq. (3), the resulting energy eigenvalue, taking into consideration that t is negative, is

$$\frac{E(\vec{k})}{|t|}=-\cos k_x-\cos k_y-\cos k_z \mp(\cos^2 k_x+\cos^2 k_y+\cos^2 k_z-\cos k_x\cos k_y-\cos k_y\cos k_z-\cos k_z\cos k_x)^{1/2}.\qquad(7)$$

At $\cos k_x=\cos k_y=\cos k_z=1$, the energy is minimum, $E(\vec{k}=0)=-3|t|$, the state being doubly degenerate. Although the actual spin arrangement is not FM, the result $|3t|$ sets a useful scale for the maximal energy gain from electron delocalization. Also, the dispersion relation (7) can be fitted to a FM $CaMnO_3$ majority-spin band structure calculated in density-functional theory,[16] determining the hopping energy $t=-0.75$ eV.

For light doping, the magnetic energy Eq. (5) of antiferromagnetic order ($-zJNS^2/2$ for classical spins; N is the number of Mn ions) is much larger than the hopping energy. As discussed by de Gennes,[23] the best uniform solution (for a one-band model) is a compromise where antiferromagnetic spins cant uniformly toward FM solutions. Start from the Néel AF structure and let all spins tilt towards the $\hat{x}$ direction with angle $\theta/2$, as shown in Fig. 1. This costs magnetic energy $\Delta E_J=zNJS^2(1-\cos\theta)/2$. A doped-in electron can now delocalize, reducing its energy by $-3|t|\sin(\theta/2)$. For small doping $x=n/N\ll1$, the total hopping energy is $\Delta E_t=-3n|t|\sin(\theta/2)$. Therefore when $\sin(\theta/2)=x|t|/4JS^2$, the total energy $\Delta E=\Delta E_J+\Delta E_t$ is minimum, $-3Nx^2t^2/8JS^2$. From this estimate, the system cants all the way to FM when the optimal θ equals π, which occurs at $x=4JS^2/|t|\simeq0.025$.

Because the doubly degenerate E_g electrons hop anisotropically, a better canted solution exists. Let all spins with $\exp(i\vec{K}\cdot\vec{l})=1$ [$\vec{K}$ is $(0,\pi,\pi)$] tilt towards $+\hat{x}$ and all spins

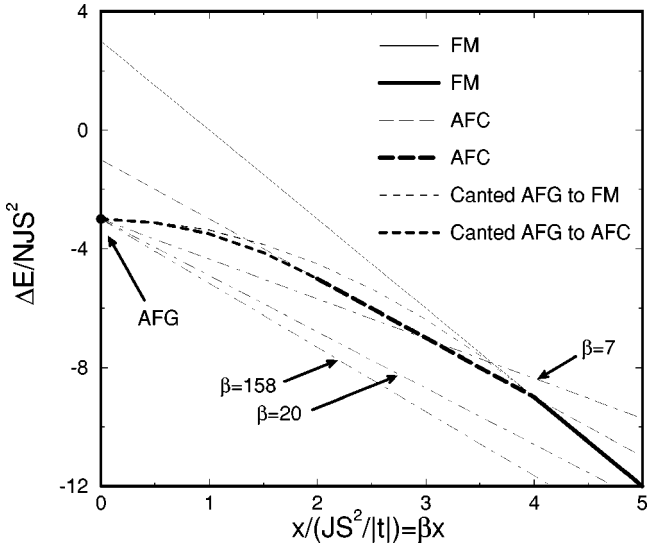

FIG. 2. Energy per electron of various doped states. Electron concentration x is measured in units of $1/\beta \equiv JS^2/|t|$. Bold lines denote the most favorable uniform states. Nonuniform (polaron) states (discussed in Sec. VI, using $\Gamma=0.25$) are denoted by dot-dashed lines for the various values of β indicated. Among different extended states, AFC lies lowest from $\beta x=2\sim4$, and FM takes over above $\beta x=4$ ($x\simeq0.025$). For light doping, the inhomogeneous polaron states are stable. As x increases, uniform states take over. The transition from polaron-doped AFG to FM occurs at $x\simeq0.045$ (using $\Gamma=0.25$, $t=0.75$ eV, $JS^2=4.74$ meV, $\beta\simeq158$). Notice that the value of β determines the critical doping x_c of the phase transition and even the transition type, as small β results in an AFG to AFC transition, rather than to FM. But for small β the predicted x_c can be large enough to exceed the light-doping approximation used here.

with an $\exp(i\vec{K}\cdot\vec{l})=-1$ tilt towards $-\hat{x}$ with an angle $\theta/2$, as shown in Fig. 1. The magnetic energy cost is reduced to $\Delta E_J=zNJS^2(1-\cos\theta)/6$, but the delocalizaton energy lowering is also reduced to $\Delta E_t=-2n|t|\sin(\theta/2)$. This type of canting terminates in C-type antiferromagnetism when $x=2JS^2/t$, as shown in Fig. 1. Figure 2 summarizes our results for the energies of uniform solutions vs x.

IV. PURE SPIN-POLARON EFFECT

Experimentally, $CaMnO_3$ is insulating at a small doping x. This rules out uniform solutions with electrons doped into delocalized states. The simplest picture is that each doped electron is localized on one Mn site, creating a local Mn^{3+} with spin $S=2$ in an AF background, for a spin excess of $\frac{1}{2}$. This does not agree with the measured saturated magnetization,[5] which has been interpreted in terms of local spin flipping (net excess spin of 2) in the region $0.02<x<0.08$. Local spin flipping leads to local FM regions (called spin polarons) around doping centers, allowing the doped electron to gain delocalization energy. In this section we discuss candidate localized ground states of a single E_g electron, using the same Hamiltonian $\mathcal{H}=\mathcal{H}_t+\mathcal{H}_J$.

First we make a continuum (effective-mass) approximation in the spirit of Nagaev.[9] Inside the local FM region, electrons hop like free electrons with inverse band mass $1/m^*=(a/\hbar)^2|t|$ given by Eq. (7), with a the perovskite lattice constant $a\simeq3.73$ Å. This electron sits in a spherical well with infinite walls at radius R, whose depth is $-3|t|$. G-type antiferromagnetism resumes for $r>R$. The ground-state energy of the electron in this polarized region is then

$$\Delta E_t=|t|\left(-3+\frac{\pi^2a^2}{2R^2}\right), \tag{8}$$

where the second term is the zero-point energy in the well. The magnetic energy cost from spin canting is

$$\Delta E_J=zJS^2(4\pi R^3/3a^3), \tag{9}$$

where the last factor is the number of Mn atoms in the cluster. Optimizing $\Delta E=\Delta E_t+\Delta E_J$ over R, the optimal size cluster has a number of Mn atoms inside the sphere equal to

$$\frac{4}{3}\pi\left(\frac{R}{a}\right)^3=\frac{4}{3}\pi\left(\frac{\pi|t|}{4zJS^2}\right)^{3/5}\simeq26. \tag{10}$$

This is close to the optimum 25-site symmetric cluster that we will find by exact diagonalization and show in Table I. However, we will also find a smaller asymmetric cluster of lower energy.

TABLE I. Ground-state energy of symmetric clusters, with only spin polaron effects included, i.e., from exact diagonalization of $\mathcal{H}_t+\mathcal{H}_J$ in the $2M$ dimensional subspace, where M is the number of Mn sites in the clusters and each Mn atom has two relevant E_g orbitals. The 25-site cluster gives the lowest ground-state energy. The last column uses $t=-0.75$ eV and $JS^2=4.74$ meV.

Cluster size M	Number of spins flipped	Energy gain from hopping ($\|t\|$)	Ground-state energy (eV)
1	0	0	0
7	1	$-\sqrt{3}=-1.732$	−1.242
25	6	−2.330	−1.406
51	13	−2.449	−1.097
57	14	−2.380	−0.989
63	19	−2.600	−0.869

It is interesting that continuum theory gives a lower energy if the region $r<R$ is canted rather than fully FM. The A sublattice is fixed for all r, but the B sublattice is tilted toward the A sublattice by an angle θ for $r<R$. Then the optimum tilting angle is 180° (FM) for $\beta=t/JS^2>\beta_c=(7\pi^2/18)^{5/2}4z/\pi\simeq220$, while for smaller β, the optimal tilting angle is $\sin(\theta/2)=\beta/\beta_c$. Our estimated value is $\beta\simeq158$, which gives $\beta/\beta_c\simeq0.72$. So the spins inside radius R are approximately 90° apart, and the optimum cluster size increases to 31.

Now we repeat the calculation using the true discrete Hamiltonian. First consider flipping only one spin. In this way, the spin-flipped Mn (the central site), along with its six nearest neighbors, form a seven-site cluster with all seven spins parallel. The cluster is invariant under transformations of the point group O_h. If the central Mn spin is kept un-

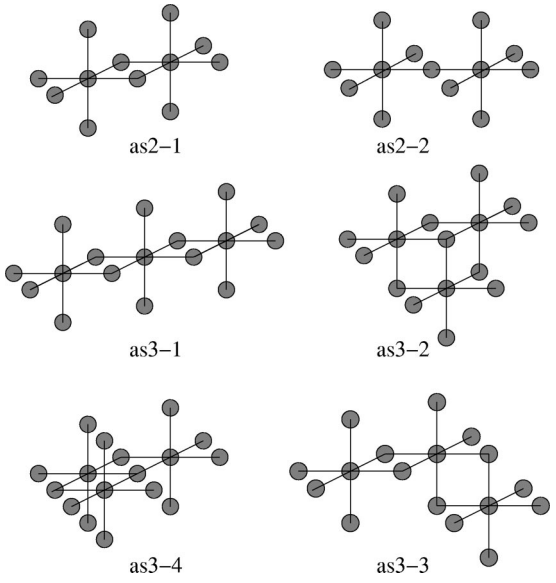

FIG. 3. Different asymmetric clusters: as2-1 and as2 have two spins flipped; the four types of as3 have three spins flipped.

flipped, but instead the spins of those six nearest neighbors are flipped, a 25-site O_h-symmetric cluster is formed. Similar steps can be taken to obtain larger and larger symmetric clusters. We will not look at candidate states with canted spins except for one special case to be mentioned later.

Each spin flip costs magnetic energy $6\times 2JS^2$. Since spins are parallel inside the cluster, the electron can hop among the E_g orbitals of all the spin-aligned Mn ions, with a corresponding energy lowering from delocalization. Table I shows numerical values of ground-state energy found by exact diagonalization of $2M\times 2M$ Hamiltonian matrices for symmetric clusters of M Mn atoms, ranging in size from $M=1$ to 63. The ground states are all doubly degenerate (E_g representation) because of the O_h symmetry of the cluster.

Asymmetric clusters are also possible. If we flip one spin at site $\vec{l}$ and another one at site $\vec{l}+\hat{x}+\hat{y}$, a 12-site cluster is formed. Starting from this 12-site cluster, there are four different ways to create a larger cluster with one more flipped spin, as shown in Fig. 3. Other possibilities are less closely packed, such as the 13-site cluster shown in the figure, and other 3-spin-flipped cases not shown here. The ground-state energy of these examples are calculated, as shown in Table II. For our chosen values of t and JS^2, the most favorable spin polaron is an asymmetric 17-site cluster with three flipped spins.

There are many possible variations with inhomogeneously canted spins, of which we considered only one, a 25-site cluster with the seven inner atoms canted rather than ferromagnetically aligned with the outer 18 atoms. This interpolates between the seven- and the 25-atom cluster. Without canting, the seven- and 25-atom cluster become equal in energy for the value $|t|/JS^2\simeq 100$, smaller than our preferred value of 158. It turned out that in the range $94<|t|/JS^2<104$, the locally canted state was lower in energy than either the seven- or the 25-atom pure ferromagnetic cluster.

TABLE II. Ground-state energy of asymmetric clusters, with only spin-polaron effects included. The as3-4 cluster gives an even lower ground-state energy than the 25-site cluster shown in Table I.

Cluster size M	Number of spins flipped	Energy gain from hopping ($\|t\|$)	Ground-state energy (eV)
12 (as2-1)	2	−1.936	−1.338
13 (as2-2)	2	−2	−1.386
16 (as3-2)	3	−2.015	−1.341
17 (as3-1)	3	−1.936	−1.281
17 (as3-3)	3	−1.984	−1.317
17 (as3-4)	3	−2.145	−1.438

V. LATTICE POLARON EFFECT

The degenerate ground state, found in the previous section for symmetrical spin polarons, is Jahn-Teller (JT) unstable.[24] We now add to our Hamiltonian lattice distortions, controlled by the electron-phonon interaction. The only lattice degrees of freedom included are oxygen motions along the bonds to the nearest two Mn ions. If an oxygen moves along this bond a distance u, it gets closer to one Mn atom and farther from another. This will raise by gu (for the closer Mn) or lower by gu (for the farther Mn) the energy of any occupied Mn E_g state of the type that points toward the oxygen (that is, the $3z^2-r^2$ state if oxygen motion in the $\hat{z}$ direction is considered.) We use adiabatic approximation (oxygen mass $\rightarrow\infty$) and treat the oxygen distortions as classical parameters. Each Mn ion is surrounded by six oxygens whose distortion amplitudes $[u_\delta(\vec{l}\pm\hat{\delta}/2),\hat{\delta}=\hat{x},\hat{y},\hat{z}]$ form basis vectors for a representation of O_h, namely, $a_{1g}\oplus e_g\oplus t_{1u}$. The vector representation t_{1u} contains the distortions $u_z(\vec{l}+\hat{z}/2)+u_z(\vec{l}-\hat{z}/2)$, etc. The remaining three degrees of freedom $[Q_z=u_z(\vec{l}+\hat{z}/2)-u_z(\vec{l}-\hat{z}/2)$,etc.] form basis vectors of a_{1g} $[Q_1=(Q_x+Q_y+Q_z)/\sqrt{6}]$ and e_g $[Q_2=(Q_x-Q_y)/2, Q_3=(2Q_z-Q_x-Q_y)/\sqrt{12}]$, in Van Vleck notation.[25] The oxygen distortions are limited by a harmonic restoring force, e.g., $-Ku_z(\vec{l}\pm\hat{z}/2)$.

The lattice elastic energy and electron-phonon interaction terms of the Hamiltonian are[26]

$$\mathcal{H}_{\rm L}=\frac{K}{2}\sum_{\vec{l}}\left[u_x\left(\vec{l}+\frac{1}{2}\hat{x}\right)^2+u_y\left(\vec{l}+\frac{1}{2}\hat{y}\right)^2+u_z\left(\vec{l}+\frac{1}{2}\hat{z}\right)^2\right], \tag{11}$$

$$\mathcal{H}_{\rm ep}=-\frac{4g}{\sqrt{3}}\sum_{\vec{l}}\left[c_z^\dagger(\vec{l})c_z(\vec{l})Q_z(\vec{l})\right. \\ \left.+\text{rotations to }\hat{x},\hat{y}\text{ directions}\right]. \tag{12}$$

$\mathcal{H}_{\rm ep}$ can be split into two parts, JT and ''breathing:''

$$\mathcal{H}_{\rm ep}=\mathcal{H}_{\rm JT}+\mathcal{H}_{\rm br}, \tag{13}$$

where, in Van Vleck notation,

$$\mathcal{H}_{\rm JT}=2g\sum_{\vec{l}}\ [c_2^{\dagger}(\vec{l})c_3^{\dagger}(\vec{l})]\begin{pmatrix} Q_3(\vec{l}) & Q_2(\vec{l}) \\ Q_2(\vec{l}) & -Q_3(\vec{l})\end{pmatrix}\begin{pmatrix} c_2(\vec{l}) \\ c_3(\vec{l})\end{pmatrix}, \tag{14}$$

$$\mathcal{H}_{\rm br}=-2\sqrt{2}g\sum_{\vec{l}}\ Q_1(\vec{l})(c_2^{\dagger}(\vec{l})c_2(\vec{l})+c_3^{\dagger}(\vec{l})c_3(\vec{l})). \tag{15}$$

The vector distortions (t_{1u}) do not couple to E_g electron states and therefore do not appear.

A simple case shows how $\mathcal{H}_{\rm JT}$ splits energy degeneracy. Suppose a doped electron is localized at a single Mn site, with no hopping or spin flipping considered. The two E_g states at that Mn are the only degrees of freedom for the electron and are originally degenerate. When the six surrounding oxygen distortions are considered, the degeneracy is lifted in $\mathcal{H}_{\rm JT}$:

$$\mathcal{H}_{\rm JT}=2g(c_2^{\dagger}c_3^{\dagger})\begin{pmatrix} Q_3 & Q_2 \\ Q_2 & -Q_3\end{pmatrix}\begin{pmatrix} c_2 \\ c_3\end{pmatrix} \tag{16}$$

$$=2g\begin{pmatrix}\alpha^{\dagger} & \beta^{\dagger}\end{pmatrix}\begin{pmatrix} -Q & 0 \\ 0 & Q\end{pmatrix}\begin{pmatrix}\alpha \\ \beta\end{pmatrix}, \tag{17}$$

where

$$\begin{pmatrix}\alpha^{\dagger} \\ \beta^{\dagger}\end{pmatrix}=\begin{pmatrix} \cos\frac{\phi}{2} & -\sin\frac{\phi}{2} \\ \sin\frac{\phi}{2} & \cos\frac{\phi}{2}\end{pmatrix}\begin{pmatrix} c_2^{\dagger} \\ c_3^{\dagger}\end{pmatrix}$$

and $(Q_2,Q_3)=Q(\sin\phi,\cos\phi)$. The change in energy due to $\mathcal{H}_{\rm JT}+\mathcal{H}_{\rm br}+\mathcal{H}_{\rm L}$ is $\Delta E=-2\sqrt{2}gQ_1\pm 2gQ+12(Q_1^2+Q^2)/2$. The energy splitting $\pm 2gQ$ comes only from the JT term. The optimal distortions are $Q_1=4\sqrt{2}g/K$ and $Q=4g/K$, which give the maximum energy lowering of the ground state $\Delta E=-6g^2/K$.

The angle ϕ does not enter ΔE. This continuous degeneracy can be lifted either by adding kinetic energy and quantization of lattice degrees of freedom (dynamic JT effect) or else by introducing higher-order anharmonic terms in $\mathcal{H}_{\rm ep}$.[27,28] However, later in the discussion of the seven-site cluster, we shall show how this continuous degeneracy is naturally removed by the increase of electronic and lattice degrees of freedom.

It is interesting to consider what would happen if spins were ferromagnetically ordered, so that magnetism would not assist localization. Then polaron formation can only occur through lattice distortion and is prohibited when the delocalization energy per electron is larger than the polaron energy, i.e., when $\Gamma=g^2/K|t|$ is less than a critical value close to 0.5. We believe that Γ is close to 0.25, so that in the hypothetical ferromagnetic case, polarons would not form. Antiferromagnetic confinement is needed before a lattice polaron effect occurs. $LaMnO_3$ is different in this respect; its cooperative Jahn-Teller ground state makes polaron formation easier.[11]

VI. THE SEVEN-SITE CLUSTER: SPIN AND LATTICE POLARON

With the full Hamiltonian considered, the seven-site cluster turns out to be the most important one, as shown later in this section. Only a single spin is flipped. Inhomogeneous canting will not be favored for this state. By understanding its ground state algebraically, we learn several interesting aspects of the influence of $\mathcal{H}_{\rm ep}$ in the Hamiltonian. The dimensionless parameter $\Gamma\equiv g^2/Kt$ characterizing the strength of electron-phonon coupling has a value near 0.25 for $LaMnO_3$, and we assume that the value for for $CaMnO_3$ is similar, i.e., $0.20<\Gamma<0.30$.[30,29] We will measure energies in units of $|t|$, using dimensionless lattice variables $Q'\equiv\sqrt{K/|t|}Q$. The prime in Q' is suppressed from here on.

To study the ground state of a single electron in the seven-site cluster, a 14-dimensional Hilbert space is used, consisting of atomic E_g orbitals from each of the seven Mn atoms. Later when we turn on $\mathcal{H}_{\rm ep}$, we will find that for small Γ, fewer than 14 basis functions are needed for the ground-state calculation. The 14-dimensional space can be decomposed into seven irreducible representations of point group O_h, namely, $A_{1g}\oplus A_{2g}\oplus T_{1u}\oplus T_{2u}\oplus 3E_g$. When lattice distortions are absent ($\Gamma=0,\mathcal{H}_{\rm ep}=\mathcal{H}_{\rm L}=0$), these functions diagonalize the 14-dimensional $\mathcal{H}_t$. The three E_g-type basis functions (ψ_2^+,ψ_3^+), (ψ_2^0,ψ_3^0), and (ψ_2^-,ψ_3^-) are degenerate separately with eigenvalues $+\sqrt{3}|t|$, 0, and $-\sqrt{3}|t|$. These six states, along with the A_{1g} state (with eigenvalue 0), will be the main states of interest when $\Gamma\neq 0$. All other states stay absent as long as Γ is small.

When $\Gamma\neq 0$, $\mathcal{H}_{\rm ep}$ and $\mathcal{H}_{\rm L}$ are turned on. Amplitudes of lattice distortions appear linearly in the matrix representation of $\mathcal{H}_{\rm ep}$ and quadratically in that of $\mathcal{H}_{\rm L}$. Since these lattice distortions are of order $\sqrt{\Gamma}$ when $\Gamma\ll 1$, $\mathcal{H}_{\rm ep}$ and $\mathcal{H}_{\rm L}$ can be treated as perturbations to $\mathcal{H}_t$. In the following, all lattice distortion modes will be introduced. Then second-order perturbation of the original ground states (ψ_2^-,ψ_3^-) can be expressed in terms of these modes and shows that most of these modes do not participate in the ground-state lattice distortion. This will in turn eliminate the need for considering electron states of symmetries that couple to the absent modes only. Finally, from the form of the perturbed ground-state energy, the pattern of its optimized lattice distortion will be derived and compared to the exact numerical result.

There are 36 oxygens adjacent to one or more Mn atoms in the seven-atom cluster, so there are 36 distortion parameters in $\mathcal{H}_{\rm ep}$. These can be organized into sets of basis vectors for irreducible representations of the point group O_h, namely, $3a_{1g}\oplus a_{2g}\oplus 5t_{1u}\oplus 3t_{2u}\oplus 4e_g$. The a_{1g}-type modes are denoted as (q_{i1}, where $i=1,2,3$), and the e_g-type modes are denoted as (q_{i2},q_{i3}), where $i=1,2,3,4$. The matrix elements of $\mathcal{H}_{\rm ep}$ can be reexpressed in terms of these modes, and $\mathcal{H}_{\rm L}$ is simply $\Sigma_{\rm modes}q_{\rm modes}^2/2$.

Second-order perturbation theory shows that for small Γ, many of these modes appear only quadratically with positive coefficients and hence should be optimized to 0. For larger Γ, these coefficients start to turn negative, and the corresponding distortions start to develop. The critical values are $\Gamma=0.443$ for the appearance of the t_{1u} and q_{43} distortion,

$\Gamma=1.30$ for t_{2u}, and $\Gamma=0.819$ for a_{2g} and q_{42}. It will thus happen that as Γ increases, the symmetry of the ground-state electron wave function and lattice distortion pattern is gradually lowered by the successive appearance of these distortions.

We therefore ignore the above modes for the actual range $\Gamma\approx 0.25\pm 0.05$. This eliminates the presence of electron states of A_{2g}, T_{1u}, and T_{2u} symmetry. The remaining modes are three sets of (q_{i1},q_{i2},q_{i3}), with $i=1,2,3$, of the inner, intermediate, and outer oxygen layers, respectively. Degenerate first-order perturbation theory for (ψ_2^-,ψ_3^-) shows that the ground-state energy of $\mathcal{H}_t$ splits into

$$\frac{E^{(1)}}{|t|}=-\sqrt{3}-\sqrt{\Gamma}(\sqrt{2}Q_1\mp\sqrt{Q_2^2+Q_3^2}), \tag{18}$$

$$Q_1\equiv\frac{1}{3}q_{11}+\frac{1}{6}q_{21}+\frac{1}{12}q_{31},$$

$$Q_2\equiv\frac{1}{3}q_{12}+\frac{1}{6}q_{22}+\frac{1}{12}q_{31},$$

$$Q_3\equiv\frac{1}{3}q_{13}+\frac{1}{6}q_{23}+\frac{1}{12}q_{33}.$$

Thus at first order, there is still a continuous degeneracy, in the sense that the energy JT splitting depends only on $Q\equiv\sqrt{Q_2^2+Q_3^2}$, not on $\phi\equiv\tan^{-1}(Q_3/Q_2)$.

To include second-order perturbations, for simplicity, we treat analytically only the distortion modes from the inner oxygen layer (q_{11},q_{12},q_{13}). The number of related electronic states is now reduced to five, namely, $(A_{1g},\psi_2^+,\psi_3^+)$ and (ψ_2^-,ψ_3^-). In this five-dimensional subspace, the Schrödinger equation to be solved can be expressed as follows (not including $\mathcal{H}_{\rm L}$, which is always proportional to the identity matrix):

$$\begin{pmatrix}\mathcal{H}_t^{II}+\mathcal{H}_{\rm ep}^{II}-E & h_{\rm ep}\\ h_{\rm ep}^T & \mathcal{H}_t^I+\mathcal{H}_{\rm ep}^I-E\end{pmatrix}\begin{pmatrix}\Psi^{II}\\ \Psi^I\end{pmatrix}=0, \tag{19}$$

where $\Psi^I\equiv(\psi_2^-,\psi_3^-)$ and $\Psi^{II}\equiv(A_{1g},\psi_2^+,\psi_3^+)$. We obtain an effective Hamiltonian $\mathcal{H}_{\rm eff}=\mathcal{H}_t^I+\mathcal{H}_{\rm ep}^I-h_{\rm ep}^T(\mathcal{H}_t^{II}+\mathcal{H}_{\rm ep}^{II}-E)^{-1}h_{\rm ep}$ for Ψ^I. Since E should be very close to $-\sqrt{3}|t|$ for small perturbation, we take E as $-\sqrt{3}|t|\times\mathbf{1}_{(3\times 3)}$ and ignore $\mathcal{H}_{\rm ep}^{II}$ in the denominator. The $\mathcal{H}_{\rm eff}$ obtained this way shows that the degeneracy of (ψ_2^-,ψ_3^-) is now lifted to become (including $\mathcal{H}_{\rm L}$)

$$\frac{E^{(2)}}{|t|}=-\sqrt{3}-\sqrt{2}A-\left(\frac{4\sqrt{3}}{3}-\frac{9}{2\Gamma}\right)(A^2+\rho^2)\pm\sqrt{\epsilon},$$

$$\epsilon\equiv\frac{4}{3}\rho^4+\frac{32}{3}A^2\rho^2+\frac{8\sqrt{6}}{3}A\rho^2+\rho^2$$

$$+\frac{4}{3}\rho^3(4\sqrt{2}A+\sqrt{3})\cos(3\theta), \tag{20}$$

where we introduce the notation

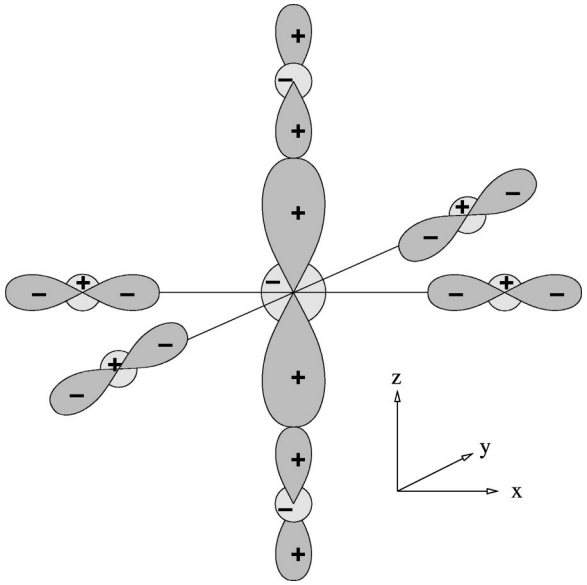

FIG. 4. One of the possible ground-state wave functions in the seven-site cluster. The corresponding lattice distortion pattern has q_1 and q_3 components.

$$A\equiv\frac{\sqrt{\Gamma}}{3}q_{11},\quad \rho\equiv\sqrt{B^2+C^2},$$

$$B\equiv\frac{\sqrt{\Gamma}}{3}q_{12}\equiv\rho\sin\theta,\quad C\equiv\frac{\sqrt{\Gamma}}{3}q_{13}\equiv\rho\cos\theta.$$

We see that $\cos 3\theta$ should be $+1$ to minimize the ground-state energy. Hence the degeneracy of ground states is not continuous anymore and has become threefold. This feature agrees with the numerical result. The ground-state electronic wave function of $\theta=0$ is shown in Fig. 4. A rotation that brings $\hat{z}$ to $\hat{x}$ $(\hat{y})$ will generate the wave functions of $\theta=2\pi/3$ $(\theta=4\pi/3)$.

VII. NUMERICAL RESULTS

Now we consider the full Hamiltonian $\mathcal{H}=\mathcal{H}_t+\mathcal{H}_J+\mathcal{H}_{\rm ep}+\mathcal{H}_{\rm L}$ for all clusters examined in Sec. IV. FM spin alignment facilitates hopping and causes energy lowering from delocalization, therefore encouraging the polaron to grow. However, as Γ increases, the JT splitting will become the dominating influence on the ground-state energy. Greater localization enhances the JT energy lowering, which increases localization of the electron. On the other hand, $\mathcal{H}_J$ and $\mathcal{H}_{\rm L}$ serve as penalties for spin misalignment and lattice distortions. Our numerical studies find the optimal resolution of the competition between these effects. The seven-site cluster becomes favored from $\Gamma>0.18$, as shown in Fig. 5. and Fig. 6. For all clusters considered, when Γ becomes large enough, the size of the ground-state wave function shrinks to become that of the seven-site polaron, as shown in Fig. 7. Enlarging the size of the FM cluster to enhance delocalization energy is then disfavored by the strong lattice polaron

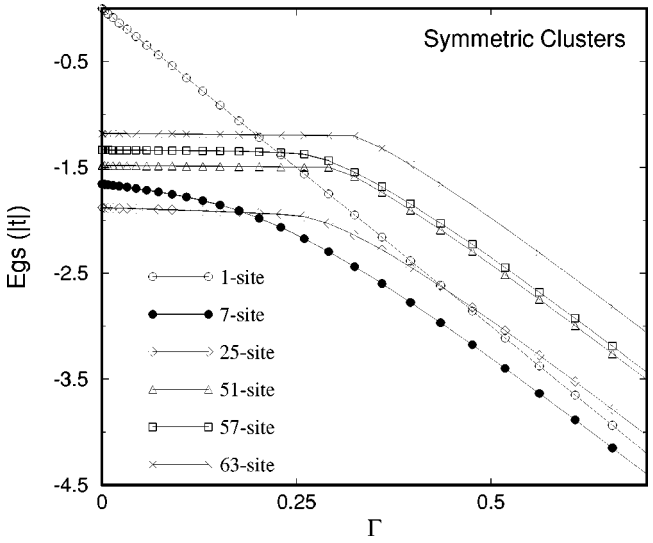

FIG. 5. Numerical results for ground-state energy (E_{gs}) of symmetric clusters, obtained by diagonalizing $\mathcal{H}_t+\mathcal{H}_J+\mathcal{H}_{\rm ep}+\mathcal{H}_{\rm L}$ in the $2M$ dimensional subspace.

effect. It is also clear that for extremely large Γ, the one-site lattice polaron will be the only form of electron state that exists.

Our numerical calculation predicts the lattice distortion pattern of the seven-site ground state. For $\Gamma=0.25$, $t=0.75$ eV, and $K=27.2$ eV/Å^2 (obtained from Raman scattering in $LaMnO_3$), the ground state shown in Fig. 4 has oxygen displacement parameters $q_{11}\simeq 1.1$, $q_{13}\simeq 0.78$, and $q_{12}=0$, which gives an outward displacement of 0.15 Å in the $\hat{z}$ direction and smaller outward displacements of 0.036 Å in both $\hat{x}$ and $\hat{y}$ directions for the six oxygens surrounding the central Mn. Displacements of oxygens in the intermediate and outer layers are at least 10 times smaller. As predicted perturbatively, t_{1u}, t_{2u}, a_{2g}, q_{42}, and q_{43} distortions are absent.

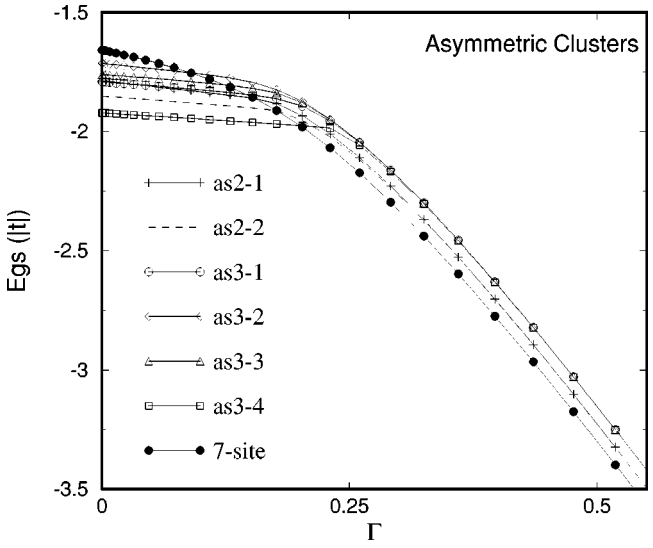

FIG. 6. Numerical results for ground-state energy (E_{gs}) of asymmetric clusters, obtained by diagonalizing $\mathcal{H}_t+\mathcal{H}_J+\mathcal{H}_{\rm ep}+\mathcal{H}_{\rm L}$ in the $2M$ dimensional subspace. The symmetric seven-site cluster is also shown here as it becomes the optimal solution when Γ exceeds 0.2.

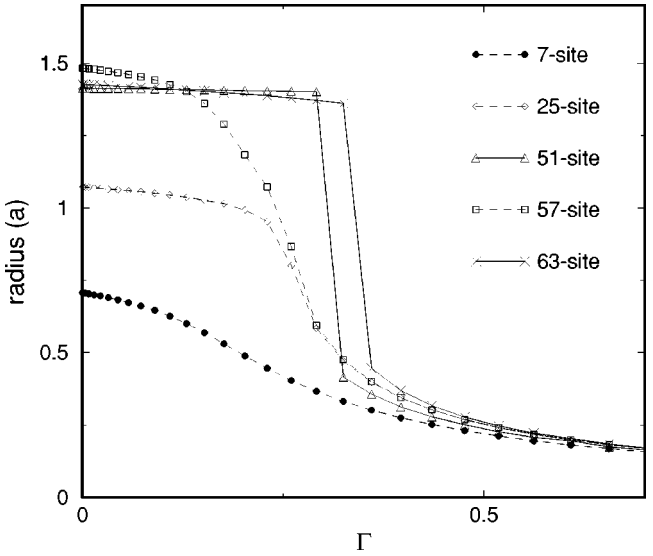

FIG. 7. Numerical results for the ground-state radius of symmetric clusters. The radius is measured in units of lattice constant a (the Mn-Mn separation distance) and is defined to be $[\Sigma_i(\vec{r}_i-\langle\vec{r}\rangle)^2\psi_i^2]^{1/2}$, where the index i runs over all Mn sites inside the cluster, and $\langle\vec{r}\rangle\equiv\Sigma_i\vec{r}_i\psi_i^2$.

VIII. TWO-ELECTRON PROBLEM

When two electrons are too close to be considered isolated, it is interesting to see if they form a bipolaron. Without introducing additional parameters in our Hamiltonian, we look at the two-electron problem for the extreme cases where the on-site Coulomb repulsion, or the Hubbard U, is 0 or ∞. Here again we consider the FM clusters mentioned earlier and look at $\Gamma=0.25$ only.

For $U=0$, the ground-state energy of a bipolaron is given when the single-electron ground state and first excited state are both occupied. With the lattice distortion re-optimized numerically, we find that the seven-site cluster has the lowest bipolaron ground-state energy, which is $0.74|t|$ lower than two separate polarons. However, when $U\rightarrow\infty$ (with no nearest-neighbor repulsion considered) in the same seven-site cluster (with lattice distortion again reoptimized) the bipolaron ground state is lifted up to become $0.86|t|$ higher than two separated polarons. We then varied U to find the critical value above which a bipolaron does not occur. Considering only the seven-site cluster, we obtain $U_c\approx 0.98|t|$, a very small value, about 0.74 eV.

For a more careful investigation, different shapes of clusters should be considered, as well as different spin orientations inside the clusters. Since bipolarons have a larger size than polarons, the variety of possible shapes and spin textures is therefore also larger. A continuum calculation similar to that in Sec. IV shows that, without electron-electron interaction, the optimal size of a FM bipolaron contains 50 Mn atoms. For a realistic theory, on-site and nearest-neighbor

Coulomb repulsions should both be included. Our results suggest that bipolarons are likely to be unstable relative to polarons, and phase separation is not likely to happen.

IX. DISCUSSION

When doping x is nonzero, one should ask whether localized polaron solutions will distribute homogeneously or will attract, causing phase separation.[31] We have not addressed this issue, which requires a more complicated calculation with additional Coulomb parameters in the Hamiltonian. Experiment is consistent with a concentration interval up to $x = 0.08$ where polarons are homogeneously distributed.[5] Our model shows that by this concentration, randomly distributed seven-site polarons will overlap significantly. However, our model also shows that at concentrations when $x > 0.045$, polarons should be unstable relative to an undistorted ground state with FM spin order and metallic conduction by the doped electrons. This effect is not seen in experiments. Apparently alternate ground states, possibly involving organization of polaronic distortions, occur and enable the system to remain nonmetallic. Without additional physics (such as defects), our model cannot account for the observation[5] that La concentrations with x less than 0.02 yield less of an excess moment than expected from seven-site polarons.

Our model describes the competing spin- and lattice polaron effects. We believe that it contains the main features needed to describe the system. A test would be measurement of the oxygen displacements, which our model predicts. The model omits nonadiabatic phonon effects, spin quantization, temperature, and polaron-polaron interactions.[32] For higher doping levels or $T > 0$, these may have a larger influence and present challenges that could be worth pursuing if experimental guidance improves.

ACKNOWLEDGMENTS

We thank J. J. Neumeier for suggesting this investigation, J. J. Neumeier and J. L. Cohn for comments on the manuscript, and V. Perebeinos and A. Abanov for discussions. This work was supported by NSF Grant No. DMR-0089492.

[1] E. O. Wollan and W. C. Koehler, Phys. Rev. **100**, 545 (1955).
[2] G. H. Jonker and J. H. van Santen, Physica (Amsterdam) **16**, 337 (1950).
[3] G. H. Jonker, Physica (Amsterdam) **22**, 707 (1965).
[4] *Colossal Magnetoresistance, Charge Ordering, and Related Properties of Manganese Oxides*, edited by C. N. R. Rao and B. Raveau (World Scientific, Singapore, 1998)
[5] J. J. Neumeier and J. L. Cohn, Phys. Rev. B **61**, 14 319 (2000).
[6] A. Maignan, C. Martin, F. Damay, B. Raveau, and J. Hejtmanek, Phys. Rev. B **58**, 2758 (1998).
[7] C. Zener, Phys. Rev. **82**, 403 (1951).
[8] P. W. Anderson and H. Hasegawa, Phys. Rev. **100**, 675 (1955).
[9] E. L. Nagaev, Zh. Éksp. Teor. Fiz., Pis'ma Red **6**, 484 (1967) [JETP Lett. **6**, 18 (1967)].
[10] K. H. Höck, H. Nickisch, and H. Thomas, Helv. Phys. Acta **56**, 237 (1983).
[11] P. B. Allen and V. Perebeinos, Phys. Rev. B **60**, 10 747 (1999); Phys. Rev. Lett. **83**, 4828 (1999); V. Perebeinos and P. B. Allen, *ibid.* **85**, 5178 (2000).
[12] J. B. Goodenough, A. Wold, R. J. Arnott, and N. Menyuk, Phys. Rev. **124**, 373 (1961).
[13] E. Fradkin, *Field Theories of Condensed Matter Systems* (Addison-Wesley, Palo Alto, 1991).
[14] S. Satpathy, Z. S. Popovic, and F. R. Vukajlovic, J. Appl. Phys. **79**, 4555 (1996).
[15] J. C. Slater and G. F. Koster, Phys. Rev. **94**, 1498 (1954).
[16] W. E. Pickett and D. J. Singh, Phys. Rev. B **53**, 1146 (1996).
[17] T. Hotta, A. L. Malvezzi, and E. Dagotto, Phys. Rev. B **62**, 9432 (2000).
[18] J. H. Jung, K. H. Kim, D. J. Eom, T. W. Noh, E. J. Choi, J. Yu, Y. S. Kwon, and Y. Chung, Phys. Rev. B **55**, 15 489 (1997).
[19] Z. Zeng, M. Greenblatt, and M. Croft, Phys. Rev. B **59**, 8784 (1999).
[20] G. S. Rushbrooke and P. J. Wood, Mol. Phys. **1**, 257 (1958).
[21] G. S. Rushbrooke and P. J. Wood, Mol. Phys. **6**, 409 (1963).
[22] M. E. Fisher, Rep. Prog. Phys. **30**, 615 (1967).
[23] P. G. de Gennes, Phys. Rev. **118**, 141 (1960).
[24] H. A. Jahn and E. Teller, Proc. R. Soc. London, Ser. A **161**, 220 (1937).
[25] J. H. Van Vleck, J. Chem. Phys. **7**, 72 (1939).
[26] There is a factor of 2 change in the normalization of the displacement variables $Q \propto u_a - u_b$ in the present paper, relative to the convention used in Ref. 11. For this reason, even though the coupling constant g is exactly the same, the Hamiltonian Eqs. (12), (14), and (15) look larger by a factor of 2. When expressed in terms of the single atom displacements u, the Hamiltonians are the same.
[27] J. Kanamori, J. Appl. Phys. **31**, 14S (1960).
[28] A. J. Millis, Phys. Rev. B **53**, 8434 (1996).
[29] Z. Popovic and S. Satpathy, Phys. Rev. Lett. **84**, 1603 (2000).
[30] Y. Okimoto, T. Katsufuji, T. Ishikawa, A. Urushibara, T. Arima, and Y. Tokura, Phys. Rev. Lett. **75**, 109 (1995).
[31] A. Moreo, S. Yunoki, and E. Dagotto, Science **283**, 2034 (1999).
[32] C. D. Batista, J. Eroles, M. Avignon, and B. Alascio, Phys. Rev. B **58**, 14 689 (1998).